Supplementary Material for

Social information use and the evolution of unresponsiveness in collective systems

Approximate analytical model of collective dynamics

To begin we first write the continuous time, one-step master equation that governs the dynamics of the population response to the environment, this is

$$\frac{dP_i(t)}{dt} = \tau^+_{i-1}(t)P_{i-1}(t) + \tau^-_{i+1}(t)P_{i+1}(t) - \tau^+_i(t)P_i(t) - \tau^-_i(t)P_i(t) \tag{1}$$

where $P_i(t)$ is the probability that i individuals are in the state $U = 1$ at time t, and $\tau^+_i(t)$ and $\tau^-_i(t)$ are the transition probabilities from i to $i + 1$ and $i - 1$ respectively, at time t.

While it is possible to solve Eqn. 1 numerically and recover the results obtained by the individual-based simulations, further analysis in this form is not possible. Instead we introduce several simplifying assumptions as follows.

Firstly we assume the system size is large and take the deterministic limit of Eqn.1. We define $X(t)$ as the average fraction of individuals in state $U = 1$,

$$X(t) = \frac{1}{N}\sum_i^N iP_i(t) \tag{2}$$

which, combining with Eqn. 1 and neglecting fluctuations leaves,

$$\frac{1}{N}\frac{dX(t)}{dt} = \tau^+(X,t) - \tau^-(X,t) \tag{3}$$

where we have redefined the transition probabilities to be functions of the continuous variable X instead of i. In deriving Eqn. 3 we have neglected the role of fluctuations on the time evolution of the mean and hence this is not a rigorous expansion of the master equation. No formal expansion is available for arbitrary transition probabilities [1] as the effect of fluctuations depends on the shape of these functions and errors are potentially unbounded. However for any given functional form of $\tau^+(X,t)$ and $\tau^-(X,t)$ there exists a sufficiently large N for which Eqn. 3 describes the time evolution of the mean fraction of individuals as computed from Eqn. 1.

Next we focus our attention on the case where the environment is defined by the square wave function. As a proxy for the full simulations in the dynamic environment we assume that all individuals are matched to the state $G = -1$ and the environment switches to the state $G = 1$ at time $t = 0$. Effectively we take this single response as a representation of the long term dynamics, which is exact in the deterministic limit, save for the assumption of the initial condition (in the full simulation the fraction of individuals at time $t = 0$ in the state $U = -1$ would be determined by the response to the previous cycle). However by making this assumption we are able to remove the explicit time dependence of the transition probabilities.

To calculate these time-independent transition probabilities, $\tau^+(X)$ and $\tau^-(X)$, we first require the probability an individual will make a correct decision (here we introduce a change of variables $\omega'_g = \omega_g/\sigma^2$),

$$P_C(X,t) = \sum_{j=0}^{k}\binom{k}{j}X^j(1-X)^{k-j}\,P(sw^+|j,\omega_s,\omega'_g,G=1) \tag{4}$$

This expression can be interpreted as the probability of firstly making j out of k observations of neighbors in the $U = +1$ state, then, secondly, switching to the state $U = +1$ given these social observations, the strategy (ω_s, ω'_g) and that the true environment is in the state $G = +1$. (This second probability is denoted by $P(sw^+|j,\omega_s,\omega'_g,G=1)$ in Eqn. 4.) The total probability is then found by summing over all possible values of j weighted by their probability of occurrence.

To relate this to $\tau^+(X,t)$ we only require that the focal individual was not already in the correct $U = 1$ state. This leads to, (dropping primes for clarity),

$$\tau^+(X) = (1-X)\sum_{j=0}^{k}\binom{k}{j}X^j(1-X)^{k-j}\,P(sw^+|j,\omega_s,\omega_g,G=1) \tag{5}$$

Similarly the probability of a transition to a less accurate collective state can be found as

$$\tau^{-}(X) = X\left(1 - \sum_{j=0}^{k} \binom{k}{j} X^{j} (1-X)^{k-j} P(sw^{+}|j, \omega_s, \omega_g, G=1)\right). \tag{6}$$

Finally, our last simplifying assumption is that k is large. In this situation the variance in the binomial distribution shrinks and the probability distribution converges to a delta function centred on the mean of kX. Hence we may replace the summation over binomial probabilities with a function of the mean of the distribution,

$$\tau^{+}(X) = (1-X)P(sw^{+}|kX, \omega_s, \omega_g, G=1). \tag{7}$$

To evaluate the probability to switch to the correct state, $P(sw^{+}|kX, \omega_s, \omega_g, G=1)$, we introduce the appropriate expression for $P(G=z)$, which in the case of the alternating step function is

$$P(G=z) = \frac{1}{2}\left[\delta(z-1) + \delta(z+1)\right], \tag{8}$$

into the optimal decision rule defined in the main text, leaving

$$U_i = \text{sign}\left[-1 + \left(\frac{e^{-\omega_g(g_i-1)^2}}{e^{-\omega_g(g_i+1)^2}}\right)\left(\frac{\omega_s}{1-\omega_s}\right)^{N^{+}-N^{-}}\right]. \tag{9}$$

Hence, individual i, will switch to $U_i = +1$ if

$$\left(\frac{e^{-\omega_g(g_i-1)^2}}{e^{-\omega_g(g_i+1)^2}}\right)\left(\frac{\omega_s}{1-\omega_s}\right)^{N^{+}-N^{-}} > 1. \tag{10}$$

As we have approximated the number of neighbors for which $U_j = +1$ as kX, the value of $N^{+} - N^{-}$ may be written as $kX - (k - kX) = k(2X-1)$, and Eqn. 10 rearranges to leave

$$e^{4\omega_g g_i} > \left(\frac{\omega_s}{1-\omega_s}\right)^{k(1-2X)}. \tag{11}$$

By taking logarithms we attain a critical value of g_i, which we denote g_c, above which the individual will switch to the state $U_i = +1$,

$$g_i > g_c = \frac{k(1-2X)}{4\omega_g} \ln\left(\frac{\omega_s}{1-\omega_s}\right). \tag{12}$$

To find the probability to switch to the correct state, $P(sw^{+}|kX, \omega_s, \omega_g, G=1)$, we require the probability that $g_i > g_c$ given $G=1$, which from the properties of the Ornstein-Uhlenbeck process is,

$$\int_{g_c}^{\infty} \sqrt{\frac{\omega_g}{\pi}} e^{-\omega_g(y-1)^2} dy = \frac{1}{2} + \frac{1}{2}\text{erf}\left[\sqrt{\omega_g}(1-g_c)\right]. \tag{13}$$

After substituting our expression for g_c, we may write the one-step transition probability of Eqn. 7 as

$$\tau^{+}(X) = (1-X)\left(\frac{1}{2} + \frac{1}{2}\text{erf}\left[\sqrt{\omega_g} + \frac{1}{2\sqrt{\omega_g}}(X-0.5)\,k \ln\left(\frac{\omega_s}{1-\omega_s}\right)\right]\right). \tag{14}$$

In this large k, large N limit Eqn. 6 similarly becomes

$$\tau^{-}(X) = X\left(\frac{1}{2} - \frac{1}{2}\text{erf}\left[\sqrt{\omega_g} + \frac{1}{2\sqrt{\omega_g}}(X-0.5)\,k \ln\left(\frac{\omega_s}{1-\omega_s}\right)\right]\right). \tag{15}$$

All combined this leads to an ordinary differential equation describing the time evolution of the population following a switch in the environmental cue as

$$\frac{dX}{dt'} = \frac{1}{2} + \frac{1}{2}\text{erf}\left[\sqrt{\omega_g} + \frac{1}{2\sqrt{\omega_g}}(X-0.5)\,k \ln\left(\frac{\omega_s}{1-\omega_s}\right)\right] - X \tag{16}$$

where t' is a time unit rescaled by the size of the population N.

[1] N. Van Kampen, *Stochastic Processes in Physics and Chemistry* (North Holland, 2007).

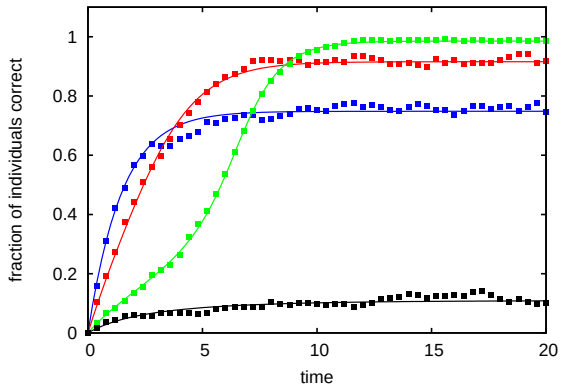

Figure S1: Time evolution of the correct opinion following an environmental switch, showing numerical solution of Eqn. 16 (lines) and individual-based simulations (points). Simulations are begun with all individuals in the incorrect state (approximating the situation immediately following an environmental transition). The time evolution of the fraction of individuals in the correct state is recorded, for the individual-based simulations points represent a single simulation. Parameters for each line are: Blue, $N = 500$, $\omega_s = 0.505$, $k = 20$; Red, $N = 1000$, $\omega_s = 0.5025$, $k = 100$; Green, $N = 2000$, $\omega_s = 0.508$, $k = 50$; Black, $N = 1500$, $\omega_s = 0.506$, $k = 80$. $\omega_g = 0.1$ for all curves.

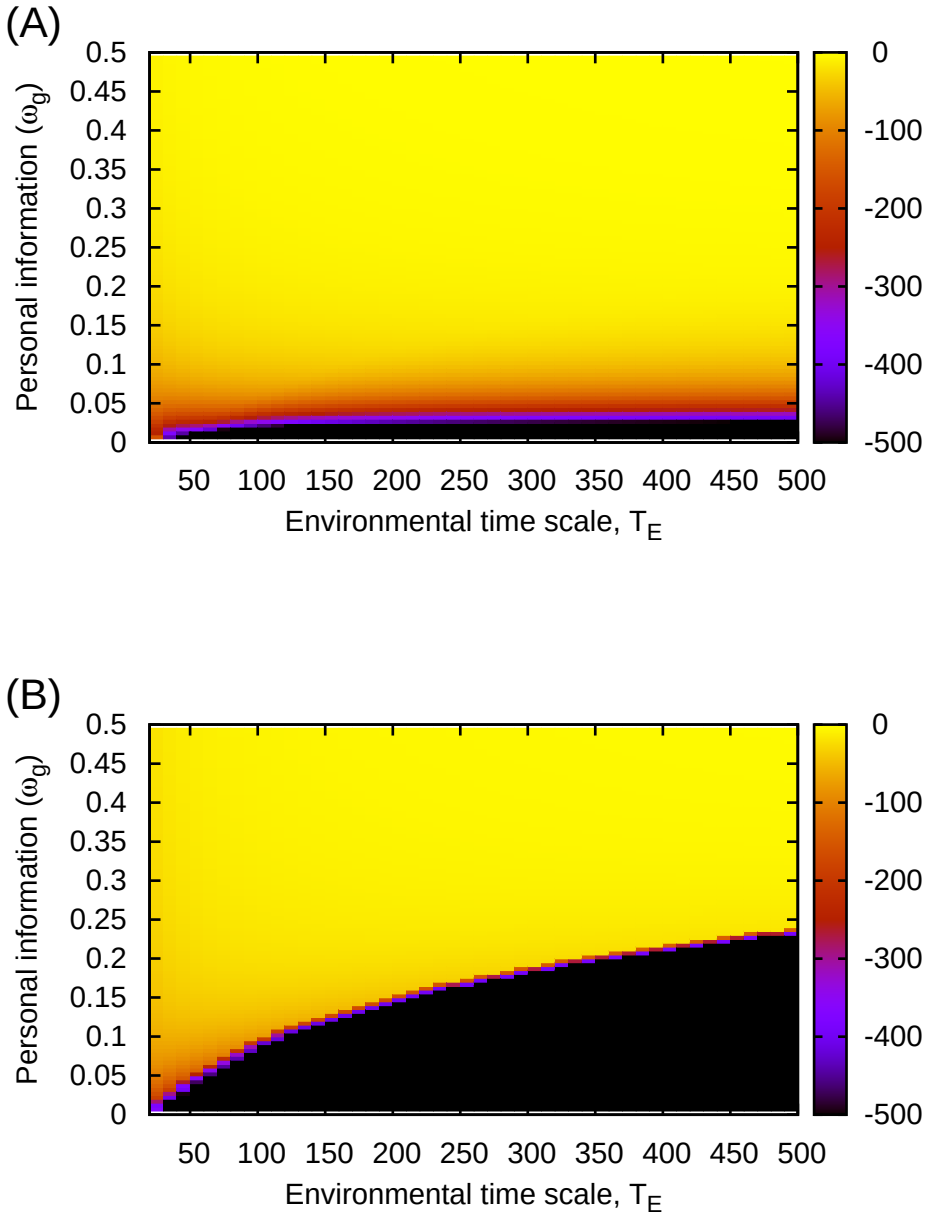

Figure S2: Evolutionary and convergence stability. (A) The condition for evolutionary stability is that the derivative of the selection gradient with respect to a rare strategy is negative at the singular strategy, i.e. $\frac{\partial^2 A(\omega_s', \omega_s)}{\partial \omega_s'^2}\Big|_{\omega_s'=\omega_s=\omega_s^*} < 0$. From numerical simulations we find that the value of the second derivative is negative throughout all parameters tested, hence no evolutionary branching occurs. (B) While simulations demonstrate the convergence of the population to the singular strategy, we include here a numerical test of the condition for convergence stability, defined as $\frac{\partial}{\partial \omega_s}\left(\frac{\partial A(\omega_s', \omega_s)}{\partial \omega_s'}\right)\Big|_{\omega_s'=\omega_s=\omega_s^*} < 0$. The derivative of the selection gradient at the singular value, with respect to the resident strategy, is negative throughout parameter space and the singular strategy is therefore convergent stable.

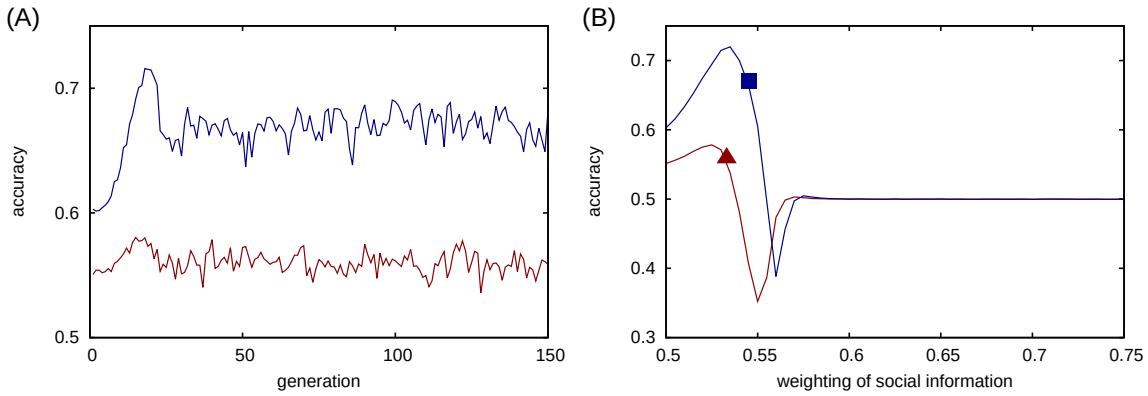

Figure S3: Simulations for rapid environmental switching. While the analytical results assume that the environment varies slowly compared to the response time of individuals, qualitatively similar results are obtained when this condition does not hold. (A) Evolution of accuracy for square wave. (B) Performance and evolved state. Different environmental time scales are shown; $T_E = 100$ blue, $T_E = 50$ red. Other parameters are $N = 100$, $\omega_g = 0.1$, $k = 8$. Faster switching reduces the ability of the group and increases the impact of a delayed response to changes (the group becomes effectively out of phase with the environment). However evolution continues to drive the system beyond the optimal value of sociality.

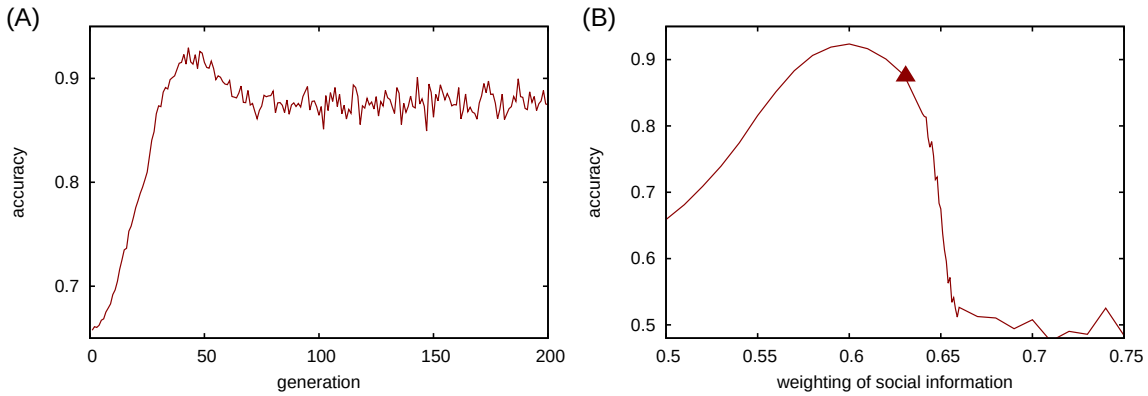

Figure S4: Simulations for random environmental switching. In previous simulations we assume the environment switches at a fixed rate, with no variance in the time between transitions. However results are not dependent on this assumption. Here the environment switches following a Poisson process with mean inter-event time of 250 (equivalent to a time scale of $\langle T_E \rangle = 500$). Other parameters are $N = 200$, $\omega_g = 0.1$, $k = 4$. (A) Evolution of accuracy for square wave. (B) Performance and evolved state.

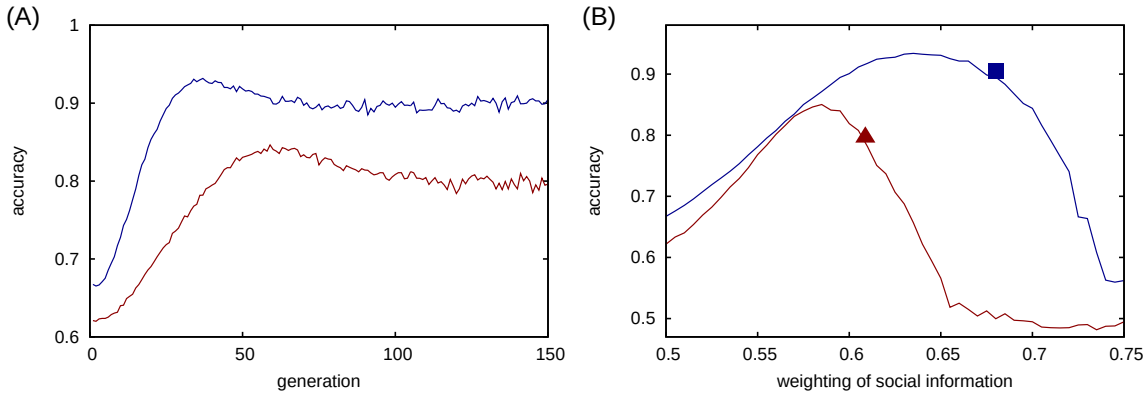

Figure S5: Varying interaction topologies: Lattice model. While analytical results assume a well-mixed population, similar effects are observed in structured networks. Here individuals interact on a 2-dimensional lattice with periodic boundaries, 4 nearest-neighbours are observed. (A) Evolution of accuracy for triangle wave (red) and square wave (blue). (B) Performance and evolved state. Parameter values are, triangle wave: $k = 4$, $N = 50$, $\omega_g = 0.2$, $T_E = 500$; square wave: $k = 4$, $N = 50$, $\omega_g = 0.1$, $T_E = 1000$. Lines represent the performance for a homogeneous population, while points show the actual ESS value to which the system evolves.

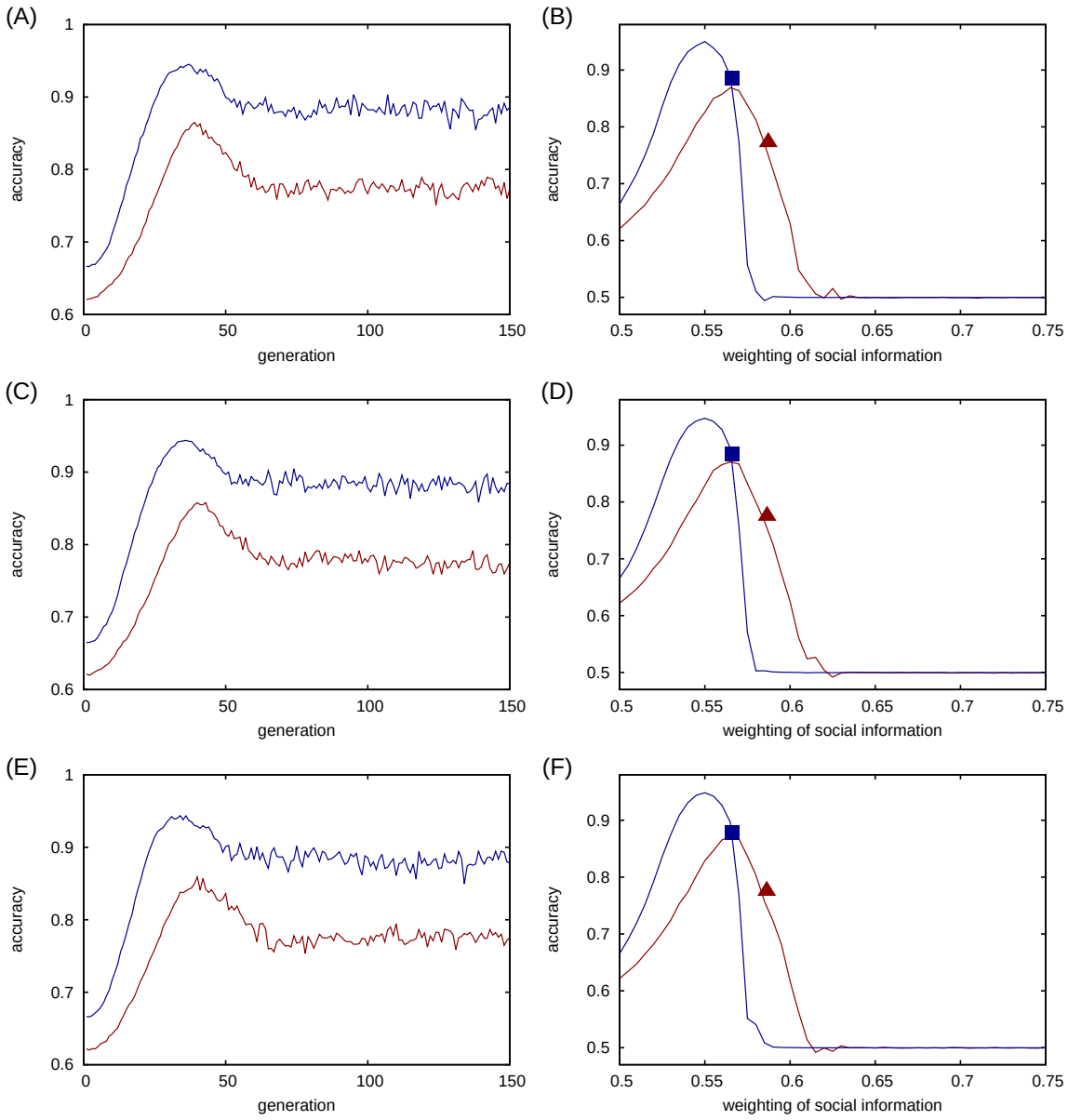

Figure S6: Random network with rewiring. In these simulations the network is unstructured however neighbours are fixed over multiple time steps. Rewiring of the network occurs intermittently, not at every time step as in the main text. (A) Evolution of accuracy for triangle wave (red) and square wave (blue). Parameter values are, triangle wave: $k = 4$, $N = 50$, $\omega_g = 0.2$, $T_E = 500$; square wave: $k = 8$, $N = 50$, $\omega_g = 0.1$, $T_E = 1000$. Rewiring occurs every $0.1T_E$ time steps. (B) Performance and evolved state. Lines represent the performance for a homogeneous population while points show the actual ESS value to which the system evolves. (C) Evolution of accuracy for triangle wave (red) and square wave (blue). Parameter values are, triangle wave: $k = 4$, $N = 50$, $\omega_g = 0.2$, $T_E = 500$; square wave: $k = 8$, $N = 50$, $\omega_g = 0.1$, $T_E = 1000$. Rewiring occurs every $0.5T_E$ time steps. (D) Performance and evolved state. Lines represent the performance for a homogeneous population while points show the actual ESS value to which the system evolves. (E) Evolution of accuracy for triangle wave (red) and square wave (blue). Parameter values are, triangle wave: $k = 4$, $N = 50$, $\omega_g = 0.2$, $T_E = 500$; square wave: $k = 8$, $N = 50$, $\omega_g = 0.1$, $T_E = 1000$. Rewiring occurs every $2T_E$ time steps. (F) Performance and evolved state. Lines represent the performance for a homogeneous population, while points show the actual ESS value to which the system evolves.

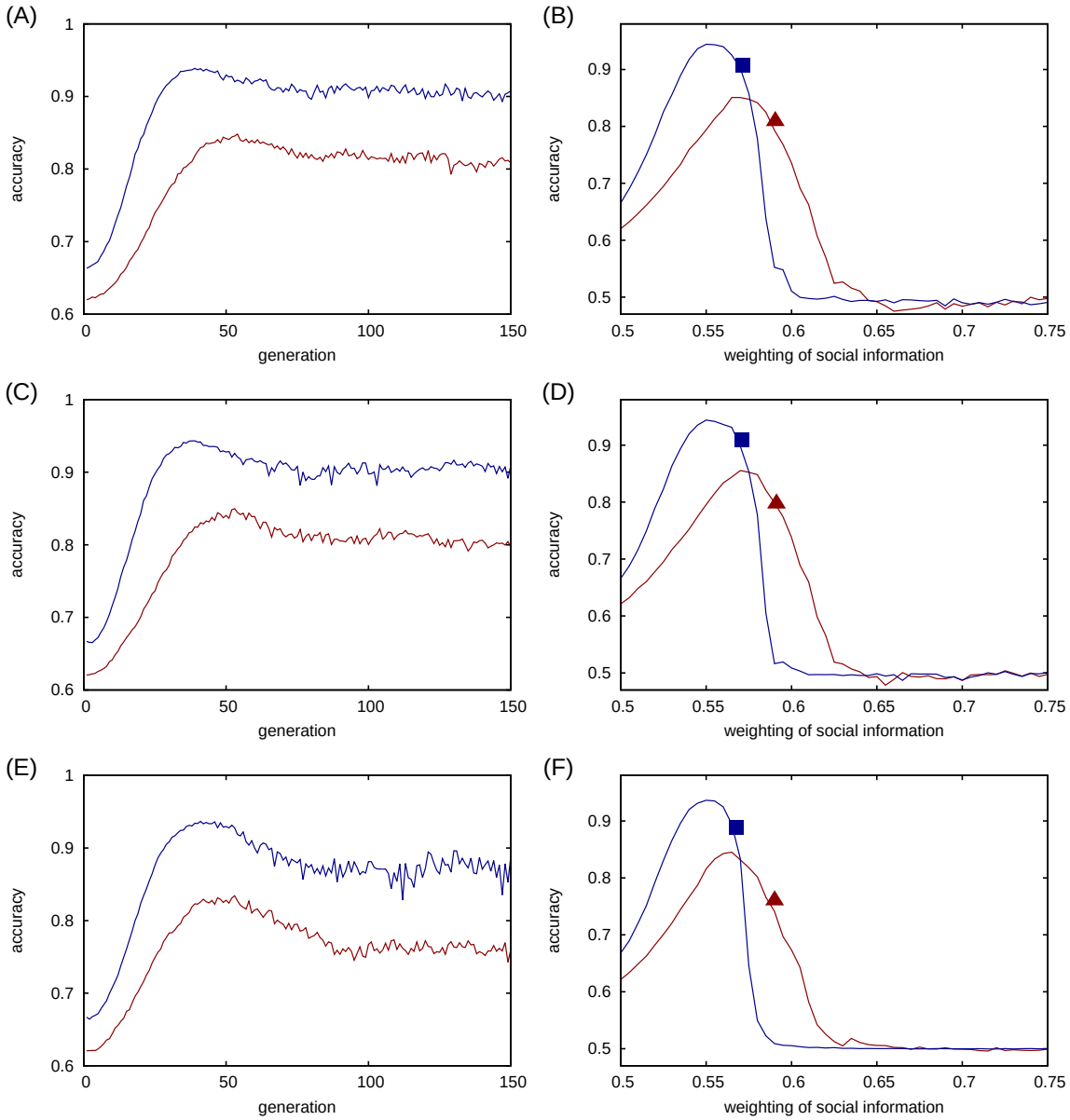

Figure S7: Small-world interaction network. (A) Evolution of accuracy for triangle wave (red) and square wave (blue). Parameter values are, triangle wave: $k = 4$, $N = 50$, $\omega_g = 0.2$, $T_E = 500$; square wave: $k = 8$, $N = 50$, $\omega_g = 0.1$, $T_E = 1000$. The network is generated through the Watts-Strogatz generation algorithm with $\beta = 0.05$. (B) Performance and evolved state. Lines represent the performance for a homogeneous population while points show the actual ESS value to which the system evolves. (C) Evolution of accuracy for triangle wave (red) and square wave (blue). Parameter values are, triangle wave: $k = 4$, $N = 50$, $\omega_g = 0.2$, $T_E = 500$; square wave: $k = 8$, $N = 50$, $\omega_g = 0.1$, $T_E = 1000$. The network is generated through the Watts-Strogatz generation algorithm with $\beta = 0.1$. (D) Performance and evolved state. Lines represent the performance for a homogeneous population while points show the actual ESS value to which the system evolves. (E) Evolution of accuracy for triangle wave (red) and square wave (blue). Parameter values are, triangle wave: $k = 4$, $N = 50$, $\omega_g = 0.2$, $T_E = 500$; square wave: $k = 8$, $N = 50$, $\omega_g = 0.1$, $T_E = 1000$. The network is generated through the Watts-Strogatz generation algorithm with $\beta = 0.8$. (F) Performance and evolved state. Lines represent the performance for a homogeneous population, while points show the actual ESS value to which the system evolves.

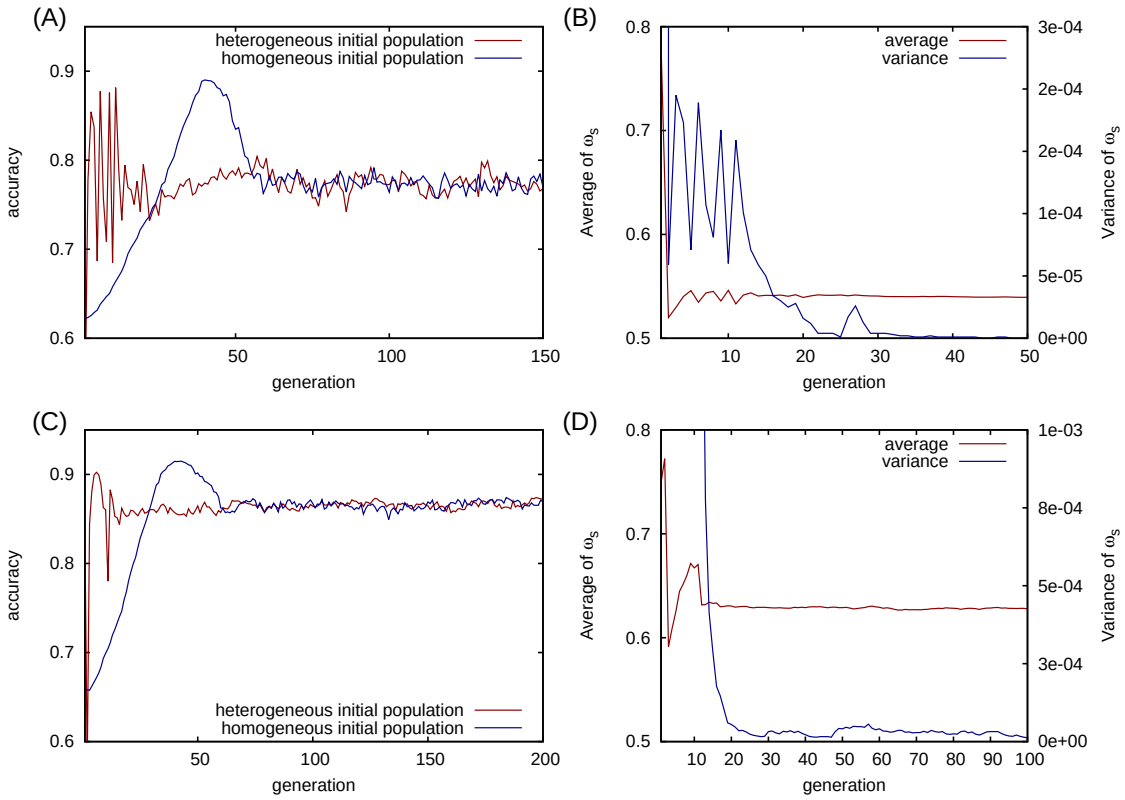

Figure S8: Evolution with heterogeneous initial populations. (A) Evolution of accuracy for triangle wave starting with uniform, randomly generated ω_s values in the interval $[0.5, 1.0]$ (red) and homogeneous population $\omega_s = 0.5$ (blue). Parameter values are $k = 8$, $N = 50$, $\omega_g = 0.2$, $\sigma = 1$, $T_E = 1000$. (B) Population variance and average values of ω_s for the simulation shown in A. (C) Evolution of accuracy for square wave starting with uniform, randomly generated ω_s values in the interval $[0.5, 1.0]$ (red) and homogeneous population $\omega_s = 0.5$ (blue). Parameter values are $k = 4$, $N = 200$, $\omega_g = 0.1$, $\sigma = 1$,$T_E = 500$. (D) Population variance and average values of ω_s for the simulation shown in C.

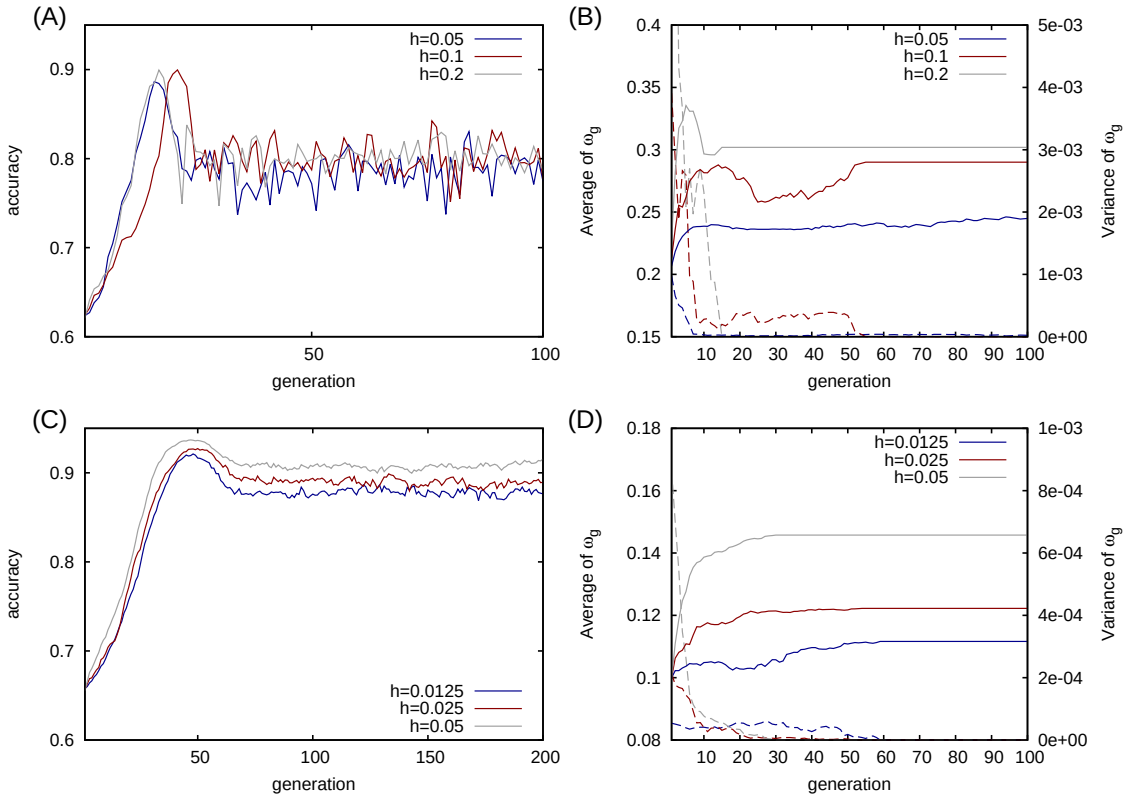

Figure S9: Evolution with heterogeneous initial populations. (A) Evolution of accuracy for triangle wave starting with uniform, randomly generated ω_g values in the interval defined by $0.2 \pm h$ where h is indicated by the legend. Parameter values are $k = 8$, $N = 50$, $\sigma = 1$, $T_E = 1000$; $w_s = 0.5$ for all individuals at the start of the simulation. Note: ω_g does not evolve. (B) Population variance and average values of ω_g for the simulation shown in A, variance is shown by dashed lines, average is shown by the solid lines. Initial variability in the population is rapidly lost and the simulation proceeds as if seeded with a homogeneous population with higher w_g value. (C) Evolution of accuracy for square wave starting with uniform, randomly generated ω_g values in the interval defined by $0.1 \pm h$ where h is indicated by the legend. Parameter values are $k = 4$, $N = 200$, $\sigma = 1$,$T_E = 500$, and $w_s = 0.5$ at the start of the simulation. (D) Population variance and average values of ω_g for the simulation shown in C, variance is shown by dashed lines, average is shown by the solid lines. Again initial variability in the population is lost but the selected strategy has a higher than average value of ω_g. Performance is therefore higher than would be observed in an equivalent, initially homogeneous population.